

Polarimetric thermal emission from periodic water surfaces

S. H. Yueh, S. V. Nghiem, R. Kwok, W. J. Wilson, and F. K. Li

Jet Propulsion Laboratory, California Institute of Technology, Pasadena, California

J. T. Johnson and J. A. Kong

Department of Electrical Engineering and Computer Science and Research Laboratory of Electronics,
Massachusetts Institute of Technology, Cambridge

Abstract. In this paper, experimental results and theoretical calculations are presented to study the polarimetric emission from water surfaces with directional features. It is observed that the measured Stokes parameters of corrugated fiberglass-covered water surfaces are functions of azimuth angles and agree very well with theoretical calculations. The theory, after being verified by the experimental data, was then used to calculate the Stokes parameters of periodic surfaces without fiberglass surface layer and with rms height of the order of wind-generated water ripples. The magnitudes of the azimuthal variation of the calculated emissivities at horizontal and vertical polarizations corresponding to the first two Stokes parameters are found to be comparable to the values measured by airborne radiometer and SSM/I. In addition, the third Stokes parameter not shown in the literature is seen to have approximately twice the magnitude of the azimuth variation of either T_h or T_v . The results of this paper indicate that passive polarimetry is a potential tool in the remote sensing of ocean wind vector.

1. Introduction

There has been an increasing interest in the microwave passive polarimetry of geophysical media [Tsang, 1991]. Theoretical calculations for the Stokes parameters of the thermal emission from periodic dielectric surfaces were carried out by Veysoglu *et al.* [1991] and were verified by the measured Stokes parameters of thermal emission from periodic soil surfaces at X band [Nghiem *et al.*, 1991]. For oceanlike rough surfaces, Monte Carlo simulations, which generate one-dimensional rough surfaces with a prescribed power law spectrum and solves the emissivities using numerical methods, were also performed [Yueh and Kwok, 1992]. All the results show that the Stokes parameters are functions of the azimuth angle between the observation direction and the corrugated direction of surfaces, suggesting that passive polarimetry may be a potential tool in the remote sensing of the ocean wind vector, which is a crucial component in the understanding of Earth climate change.

From Seasat [Jones *et al.*, 1982] in the past, ERS

1 in the present, to the NSCAT to be launched in 1996 on ADEOS platform [Naderi *et al.*, 1991], spaceborne scatterometers have been the only tool that can provide a global and frequent mapping of the ocean wind vector. The principle of wind scatterometry for detecting wind direction is based on the fact that the electromagnetic backscatter at microwave frequencies from ocean varies periodically as a function of azimuthal angle between the wind and radar look directions. This is because the sea surfaces induced by ocean wind are smoother in cross-wind direction, while rougher in upwind or downwind direction. This anisotropic directional features cause a directional dependence of microwave backscatters. Here this paper shows that the directional features of water surfaces can also affect the polarization states of thermal emission from water by ground-based Ku band radiometer measurements.

For the applications of radiometry to ocean wind field, it is known that the brightness temperatures of ocean surfaces at horizontal and vertical polarizations (T_h and T_v) correlate with wind speed over the frequency range of 1 to 40 GHz [Sasaki *et al.*, 1987]. Hence the wind speed can be inferred from the magnitude of brightness temperatures by radiometry.

Furthermore, it has been shown recently by *Etkin et al.* [1991] and *Wentz* [1992] that T_h and T_v of ocean surfaces vary as functions of the azimuth angle of observation. Etkin et al. found the dependence of brightness temperatures on the azimuth angle during circle flights using their aircraft radiometers for grazing angle ($\theta = 78^\circ$) observations with $\lambda = 1.5$ cm and nadir viewing with $\lambda = 0.8, 1.5$, and 8 cm. It was observed that the directional dependence rapidly dropped with increasing electromagnetic wavelength. Unfortunately, the measurements were not made for the middle range of incidence angles which are more important for spaceborne applications when spatial coverage and resolution need to be considered together. In the results published by *Wentz* [1992], the data investigated were collected by Special Sensor Microwave/Imager (SSM/I) which is not capable of measuring the third Stokes parameter, and after being collocated with the buoy-measured wind vectors T_h and T_v at both 19 and 37 GHz, were found to depend on wind direction with a variation of a few degrees Kelvin. The results indicate that the directional feature of water surfaces contributes to the azimuth variation of brightness temperatures. However, since the third Stokes parameter was not collected, its dependence on wind direction remains to be studied.

Previous theoretical work by *Stogryn* [1967] for emission from sea surfaces had predicted a change of a few degrees Kelvin for T_h and T_v over the azimuth angles. However, the trend of Stogryn's predictions did not seem to agree with the SSM/I data presented by *Wentz*. In Figures 2, 5, and 6 of Stogryn's paper, it was shown that the brightness temperature for horizontal polarization T_h at the upwind direction is bigger than T_h at the crosswind direction for incidence angles about 50° . In contrast, *Wentz's* model function for SSM/I, which has an incidence angle of 53° , shows the contrary. Additionally, the experimental results in this paper shows a consistent behavior with the SSM/I observations. This indicates that some further theoretical work for emission from ocean surfaces needs to be done to resolve this difference, which is not in the scope of this paper.

In view of the recent developments, ground-based radiometer measurements at Ku band and theoretical results are presented in this paper to study the azimuth dependence observed by *Etkin et al.* [1991] and *Wentz* [1992]. In addition, the third

Stokes parameter U which has not been discussed in the literature for wavy water surfaces was also measured to verify the applicability of passive polarimetry to the remote sensing of ocean wind.

As reported by *Etkin et al.* [1991] and *Wentz* [1992], T_h and T_v typically vary less than 3°K over azimuth angles. For our experimental setup, in anticipation that the expected temperature variation would be small for realistic ocean surfaces, we adopt an indirect method by performing measurements over the water surface covered by a fiberglass layer with a sinusoidal profile that provided significantly measurable brightness temperature variation over azimuth angles. The measurements were then used to verify the theory which was used to calculate the polarimetric emission parameters for such a surface profile. Once the theory was verified, we applied the theory to the surfaces with root-mean-square (rms) height in the nominal range of the roughness of wind ripples.

In section 2 the theory of polarimetric radiometry is briefly summarized, and the techniques applicable to measure the third Stokes parameter, using a linearly polarized radiometer are discussed. Section 3 summarizes the experimental setup and instrument characteristics. In addition, we compare the measurements with theory and present the theoretical Stokes parameters of polarimetric thermal emission from surfaces with realistic ripple roughness. Section 4 summarizes the results of this paper and discusses issues related to the applications of passive polarimetry to the remote sensing of ocean wind.

2. Polarimetric Radiometry

For microwave polarimetric radiometry, thermal emission is described by a Stokes vector with four parameters:

$$I = \begin{bmatrix} T_h \\ T_v \\ U \\ V \end{bmatrix} = c \begin{bmatrix} \langle E_h E_h^* \rangle \\ \langle E_v E_v^* \rangle \\ 2 \text{Re} \langle E_h E_v^* \rangle \\ 2 \text{Im} \langle E_h E_v^* \rangle \end{bmatrix} \quad (1)$$

where E_h and E_v are the horizontally and vertically polarized components of electric fields. $\langle \rangle$ denotes the ensemble average of the arguments, and c is a proportional constant [*Yueh and Kwok*, 1992]. It is known that $U = V = 0$ for geophysical media with azimuthal symmetry, while if the medium does not exhibit azimuthal symmetry, U and V are not zero

and correlate with the directional features of rough surfaces or volume anisotropic media [Yueh *et al.*, 1992].

There are two approaches which are applicable for measuring the third and the fourth Stokes parameters. One is to carry out the coherent detection of horizontally and vertically polarized electric fields and perform the complex correlation between them. The other approach carries out the power measurements at two additional polarizations, for example, a 45° linear polarization and a circular polarization. This method, which was used in our experiment, allows all of the linearly polarized radiometers to measure the third Stokes parameter by simply rotating the radiometer on the polarization plane. Specifically, the following identities are used by the second method:

$$\begin{aligned} 2 \operatorname{Re} (E_h E_v^*) &= 2|E_p|^2 - |E_h|^2 - |E_v|^2 \\ 2 \operatorname{Im} (E_h E_v^*) &= |E_h|^2 + |E_v|^2 - 2|E_c|^2 \end{aligned} \quad (2)$$

where

$$E_p = \frac{E_h + E_v}{\sqrt{2}}$$

$$E_c = \frac{E_h - iE_v}{\sqrt{2}}$$

Here E_p is the 45° linearly polarized component of the thermal emission entering the radiometer, and E_c is the circularly polarized component. Therefore four power measurements at horizontal, vertical, 45° linear, and circular polarizations allow us to generate the complete set of Stokes parameters.

Note that there are many alternatives which can be used to calculate the third Stokes parameter. For instance,

$$2 \operatorname{Re} (E_h E_m^*) = |E_p|^2 - |E_m|^2 \quad (3)$$

where E_m represents the -45° linearly polarized component; explicitly in terms of E_h and E_v ,

$$E_m = \frac{E_h - E_v}{\sqrt{2}}$$

Notice that in (3), only two linear polarizations are required, which will result in less rms uncertainty for the calculation of U than the use of (2). However, in this paper we use (2) instead of (3) because

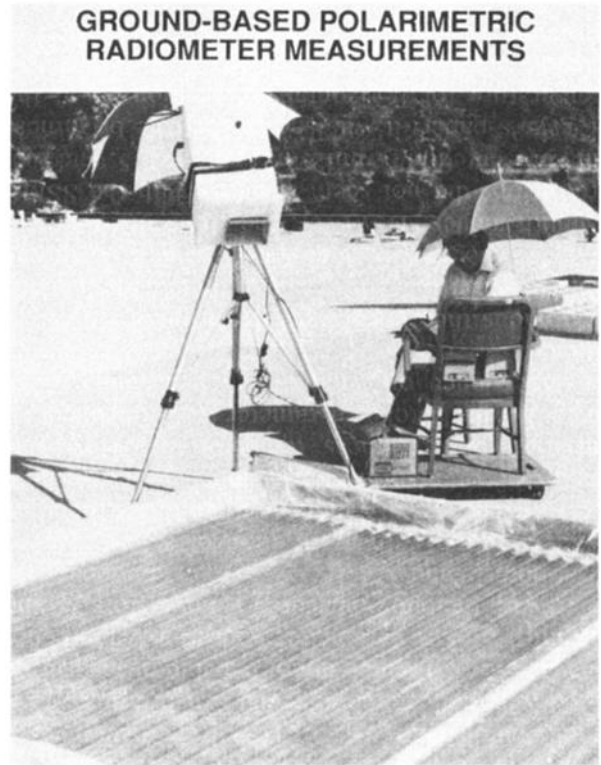


Figure 1. Experimental setup.

of our experimental limitation to be mentioned below.

3. Experimental Setup and Results

For our ground-based radiometer measurements, a water pool was constructed on the roof of a building in the Jet Propulsion Laboratory (see Figure 1 for the experimental setup). A fiberglass surface with periodic corrugations in one direction was impressed on the top of water surface to create a stationary water surface underneath it, and a plastic sheet was pasted at the edge of the fiberglass surface to prevent water from flooding the surface. The size of the surface is 8 by 8 feet which is about 4 times the footprint covered by the antenna beam. The adequacy of the surface size for the footprint coverage was checked by the invariance of the radiometer reading when absorber (radiometrically hot material) was placed along the edge of the fiberglass surface. The fiberglass surface has a sinusoidal profile with a thickness of 2 mm, a period of 6.8 cm, and a peak-to-peak height of 1.4 cm. Additionally, the dielectric constant of fiberglass was

measured to be $3.1 + i0.05$ and used in our theoretical calculations.

The radiometer used in our experiment operates at Ku band (14.6 GHz) and measures the power of a linearly polarized electric field with a rectangular horn, which has a beam width of 15° . The radiometer was mounted on a tripod at the elevation of 1.5 m above ground with a fixed incident angle at 45° . The physical limitation of the tripod prevents us from using (3). The calibration was carried out by alternately measuring the temperatures of the internal noise diode, internal noise diode plus external hot load (absorber), and the scene, resulting in an absolute accuracy of 1.5°K . The radiometer was rolled at three angular positions to measure the brightness temperatures at horizontal, vertical, and 45° linear polarizations for each azimuth angle to obtain the third Stokes parameter. Measurements over different azimuth angles was achieved by moving the radiometer around the pool and recording the relative azimuth direction of the pointing with respect to the row direction of the surface. Water temperatures were also measured to convert the measured brightness temperatures into emissivities. It was found that water temperatures reached, as high as 40°C at noon and were as low as 25°C in the morning and late afternoon. We also measured the sky temperatures, and found that the sky emissions were unpolarized and less than 3.5°K .

Figure 2 compares the measured emissivities from the fiberglass-masked water surfaces versus azimuth angles (zero when perpendicular to the row direction) with theoretical Stokes parameters. Each data point represents an average of five measurements and the error bars are included to indicate the rms errors. Measurements at some azimuth angles were repeated twice or more at different times of the day, and all data are included in Figure 2. It can be seen that the measured emissivities vary with the azimuth angles and agree reasonably well with the theoretical results obtained from the theory developed by *Johnson et al.* [1992] for a two-layer periodic dielectric surface. The theory calculates the scattered Floquet mode coefficients given an incident plane wave and derives the emissivity as one minus the reflectivity by using the Kirchhoff's law [*Peake*, 1959; *Veysoglu et al.*, 1991]. To account for the effects of finite antenna beam width, the theoretical results obtained from the plane wave illumination have been weighted by the antenna pattern for a standard gain horn over $\pm 15^\circ$ referred

to the two principal antenna polarization planes away from the boresight. Notice that we did not include the sky emission in the theoretical calculations which was considered to be negligible compared with the observed signatures.

In addition, it should be noticed that theoretical curves presented in Figure 2 are calculated using a fixed value $60 + i30$ for the dielectric constant of water, which roughly corresponds to a water temperature of 40°C according to *Klein and Swift's* [1977] formula. However, because water temperatures measured simultaneously together with brightness measurements shown in Figure 2 did vary between 25° and 40°C throughout the experiment, we further carried out a theoretical sensitivity study of water temperature effects: Theoretical emissivities are recalculated using the theoretical water dielectric constants [*Klein and Swift*, 1977] corresponding to the water temperatures measured together with the data points shown in Figure 2 and are represented by crosses in Figure 3. (In applying *Klein and Swift's* formula, the water used to fill the water tank was assumed to have a salinity of 4‰. Theoretical water dielectric constants are found to be $53 + i35$ for water temperatures at 25°C and $60 + i29$ at 40°C .) Each theoretical point signified by a cross in Figure 3 is the theoretical counterpart of a measurement data point shown in Figure 2. For easy comparison, Figure 3 includes the theoretical curves for a fixed water dielectric constant $60 + i30$ presented in Figure 2. It can be seen that the temperature variation of water dielectric constants does have some impact on the theoretical results, and the agreement between theory and measurement for vertical polarization at ϕ about 0° is degraded by comparing the small solid circles shown in Figure 2 and crosses in Figure 3. Nevertheless, its effects are small compared with the magnitude of the azimuthal variation observed in the measured brightness temperatures.

Figure 4 plots the experimental data with the theoretical results which are not averaged over antenna pattern. Notice that there are a few sharp transitions in the theoretical curves at a few azimuth angles, which are due to the change of one of the Floquet modes from evanescent to radiating or vice versa at these particular angles. As we can see that there is a dip for the emissivity of horizontal polarization at ϕ near 90° , which can also be observed in the experimental data in Figure 2 even with the averaging effects of the antenna pattern.

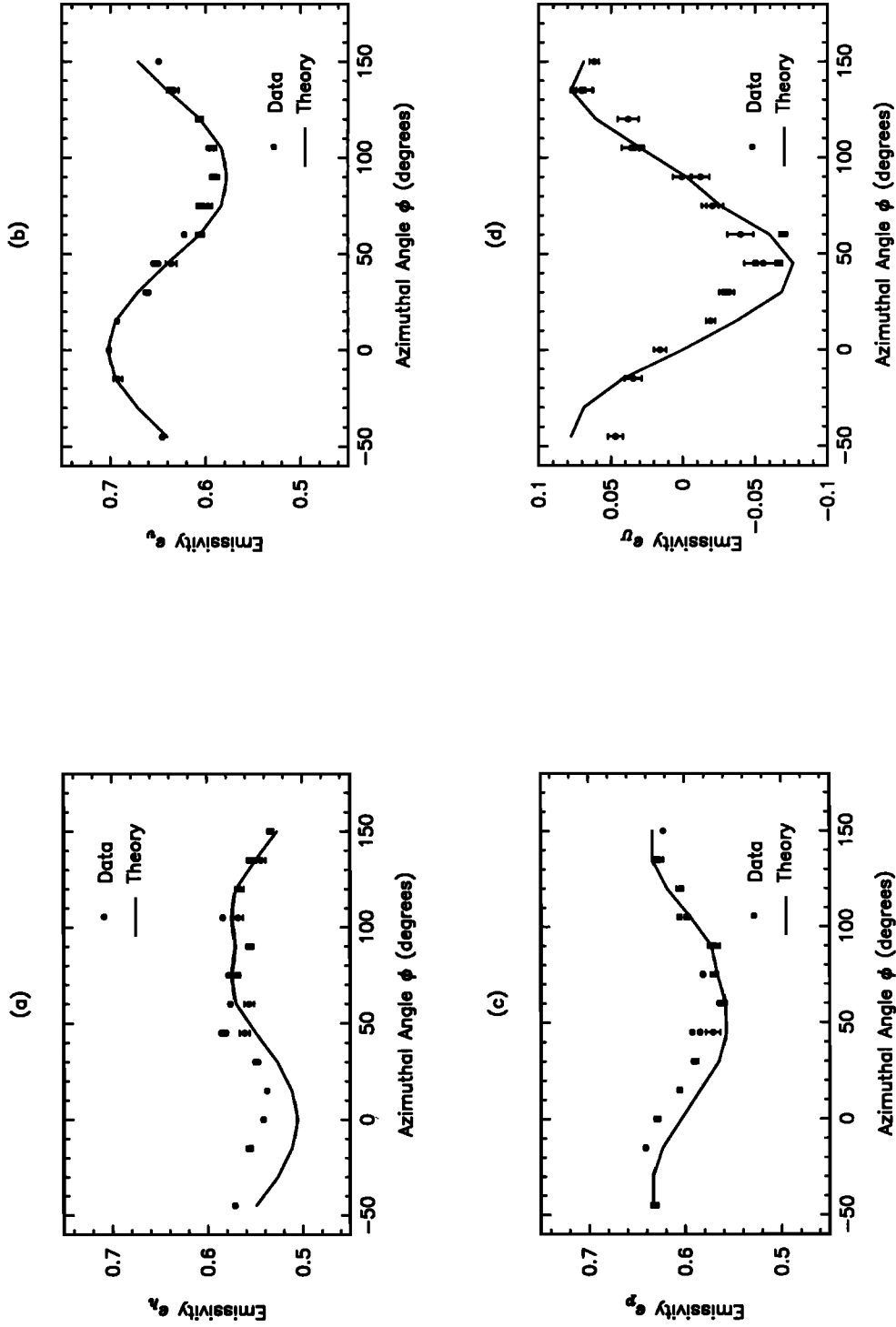


Figure 2. Comparison of measured emissivities and theoretical results with antenna pattern average. The parameters e_h , e_v , and e_p correspond to the emissivities of horizontal, vertical, and 45° polarizations, respectively, and e_u is for the third Stokes parameter U . Solid curves are the theoretical results for a fixed water dielectric constant of $\epsilon = 60 + i30$.

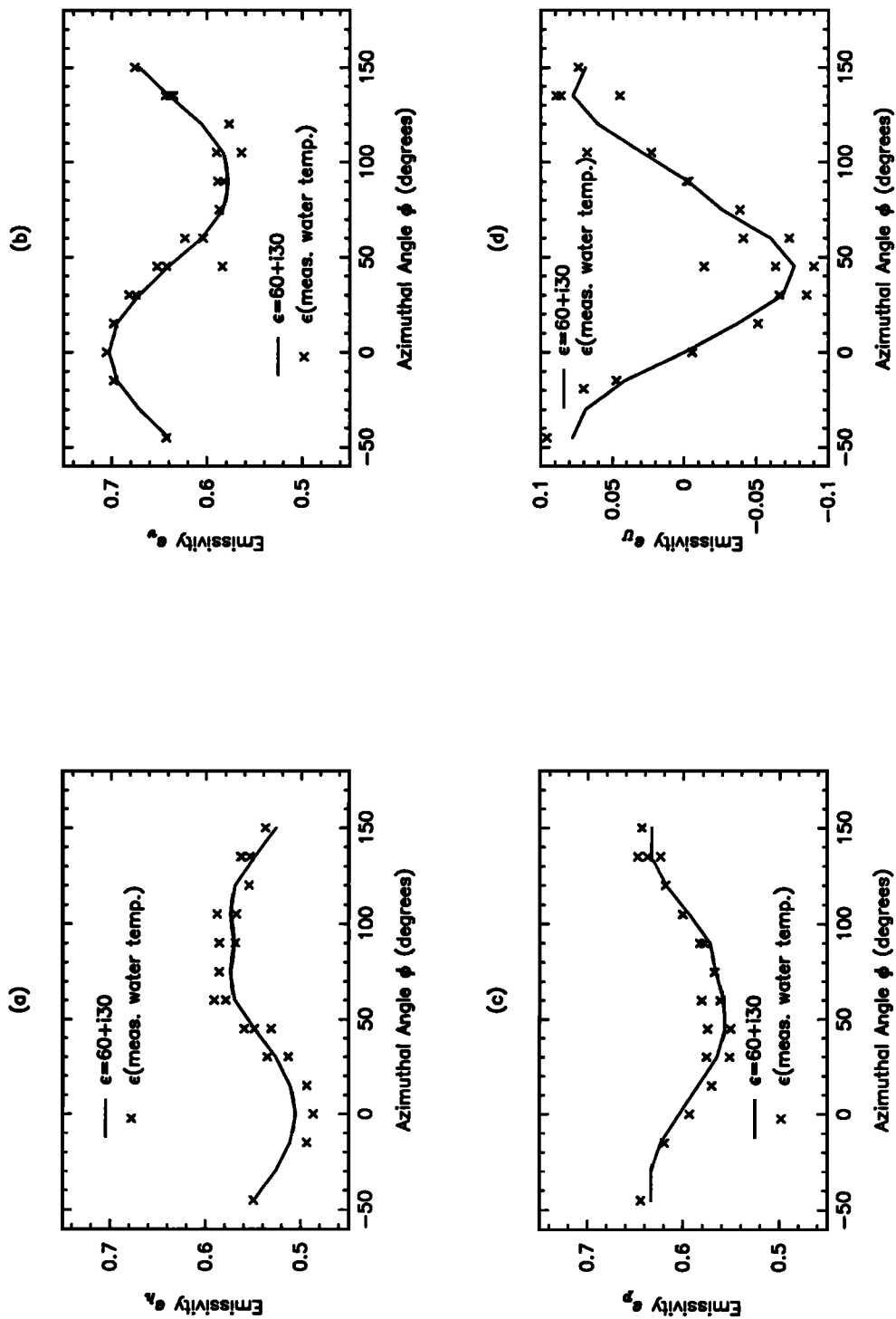


Figure 3. Sensitivity of theoretical emissivities to water temperatures. Solid curves are the theoretical results for a fixed water dielectric constant of $\epsilon = 60 + i30$. Crosses are theoretical emissivities calculated using theoretical water dielectric constants according to measured water temperatures.

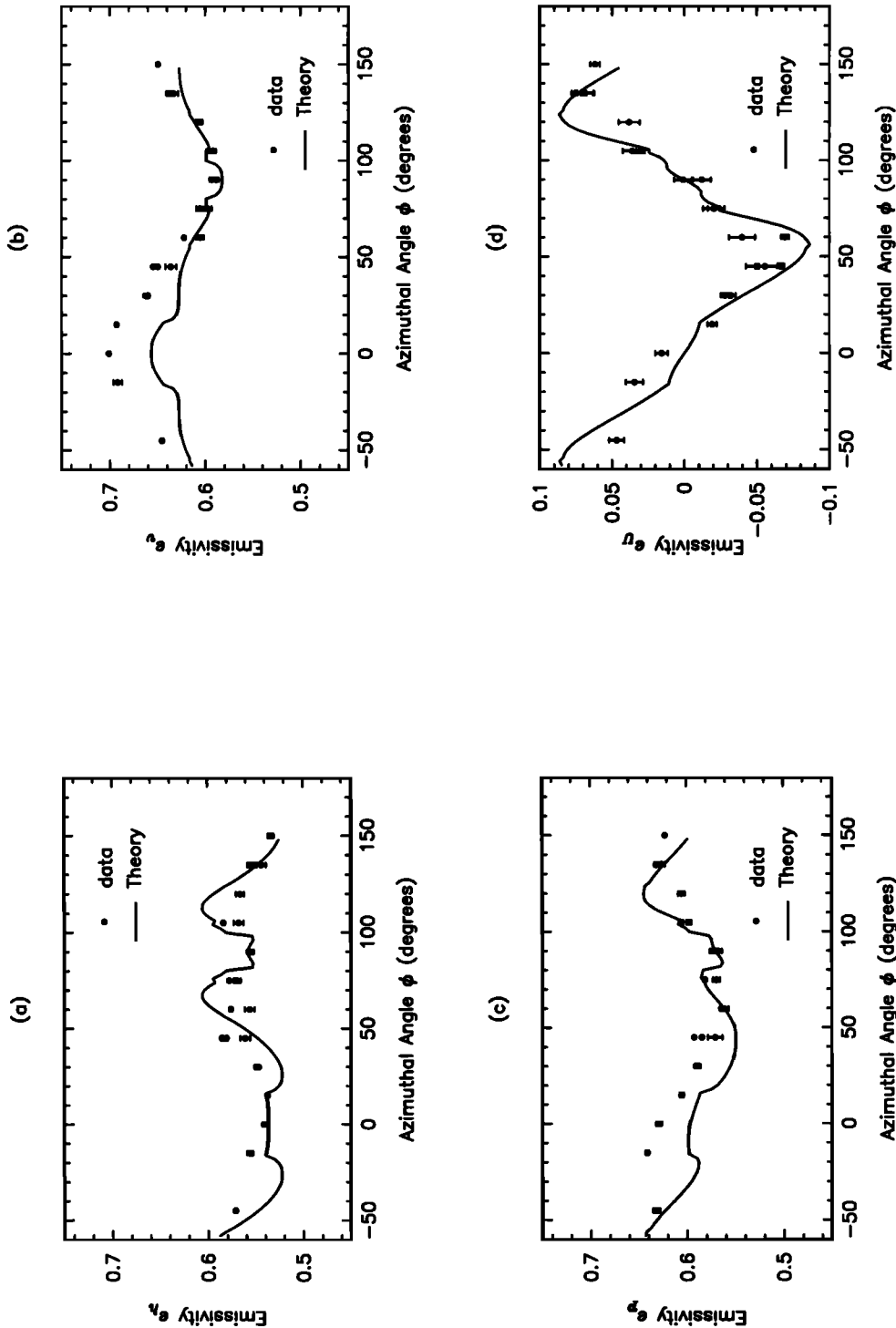


Figure 4. Theoretical results without averaging over antenna pattern and experimental data.

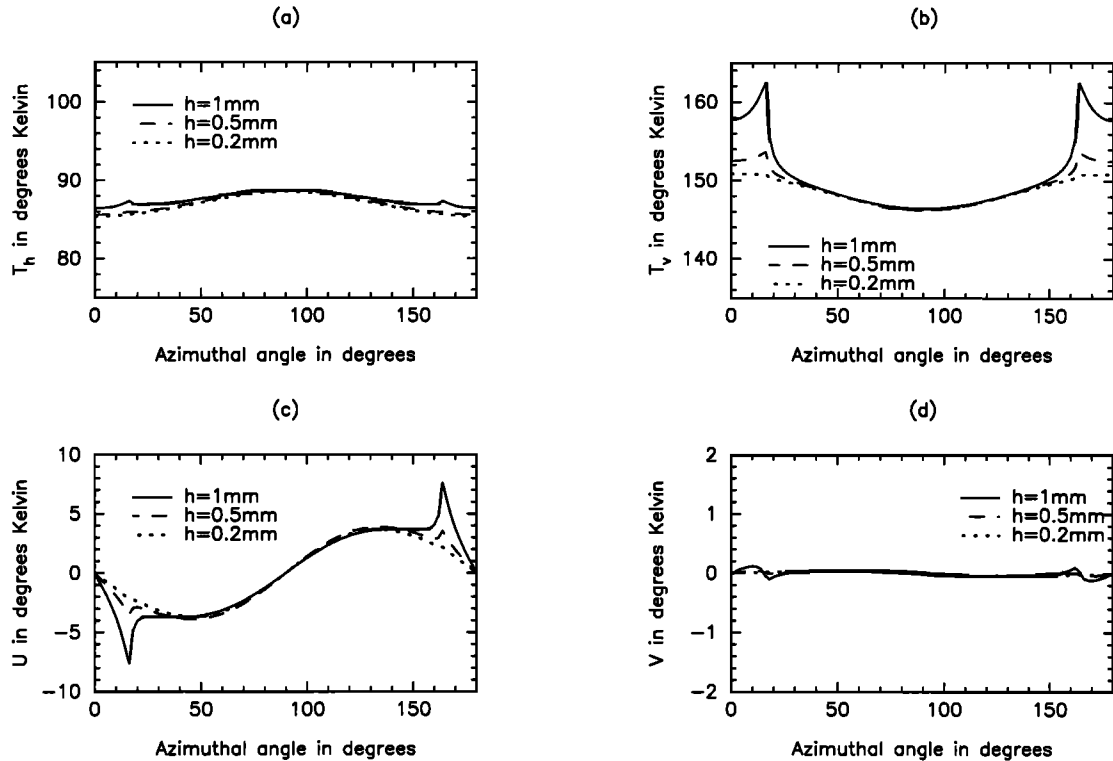


Figure 5. Brightness temperatures of sinusoidal water surfaces with height of the order of rms height of water ripples. Water dielectric constant = $57 + i32$. The physical temperature of water is assumed to be 300°K .

In the results presented above, the rms height of the sinusoidal surface is about 5 mm, which is unlikely for the rms height of short-scale wind-generated water ripples at the scale size of 6.8 cm under nominal wind conditions. Hence the magnitude of the brightness temperature variation over azimuth angles can be significantly smaller for realistic short-scale water ripples than the results shown above. Therefore theoretical calculations were further carried out for surfaces with smaller rms height.

Figure 5 illustrates the theoretical Stokes parameters for bare sinusoidal water surfaces (no fiberglass cover) with the same period of the sinusoidal corrugation as the fiberglass surface, however with smaller peak-to-peak heights ($2h$). Notice that the brightness temperatures at horizontal and vertical polarizations in Figures 5a and 5b vary by approximately 3°K over the azimuth angles, which agrees with the typical variation observed by *Etkin et al.* [1991] and *Wentz* [1992]. More interestingly is the value of the third Stokes parameter U which also

has an azimuth dependence and has a 6°K variation. In addition, it can be noticed that there are no differences for the brightness temperatures at $\phi = 0^\circ$ and $\phi = 180^\circ$ (corresponding to upwind and downwind directions) due to the symmetry of the surface with respect to row direction. Last, the fourth Stokes parameter, which cannot be measured by a linearly polarized radiometer, does not show appreciable magnitudes. However, because the sinusoidal surfaces considered here can by no means represent real ocean surfaces, which may consist of capillary waves, foams, breaking waves, and large-scale waves, such as swells, the results presented in this paper should not be overinterpreted, and the effects of these features need to be further analyzed.

4. Summary and Discussions

In this paper, results from our experiments and theoretical calculations are presented to study the polarimetric emission from water surfaces with di-

rectional features at Ku band. It is observed that the measured Stokes parameters of the fiberglass-covered water surfaces are functions of azimuth angles and agree excellently with theoretical calculations. Theoretical calculations are further extended to periodic surfaces with rms height of the order of wind-generated water ripples. The magnitudes of the azimuthal variation of the calculated emissivities at horizontal and vertical polarizations are found to be comparable to the values measured by airborne radiometer and SSM/I. In addition, the third Stokes parameter is also presented and shown to have approximately twice the magnitude of the azimuth variations of either e_h and e_v which may make it more sensitive to wind direction, while less susceptible to noises because the atmospheric and system noises tend to be unpolarized and are expected to be cancelled out when the third Stokes parameter is derived as the difference of two or three power measurements (see equations (2) and (3)). This noise problem has been observed in the results of a preliminary experiment that was carried out in the middle of August 1992 at a swimming pool. This preliminary experiment was conducted to check out the functionality of our radiometer equipment. Because of the surrounding trees and buildings, which are very hot radiometrically, we found that the measured T_h , T_v , and T_p were typically 20° above theory caused by the background noises. However, the values of the third Stokes parameter observed were very close to the results reported in this paper.

The results of this paper indicate that the passive polarimetry is a potential technology in the remote sensing of ocean wind vector. However, several issues not addressed in this paper need to be further investigated by either more accurate measurements and more extended theoretical analysis. First of all, it is known that wind-generated ocean surfaces are random and have two-dimensional directional features, unlike the one-dimensional periodic surfaces investigated in this paper. In this regard, experiments should be carried out for real ocean surfaces with various wind conditions. Furthermore, theoretical calculations should be extended to two-dimensional random rough surfaces and are currently under investigation. The second issue is the selection of the frequency band of the radiometer measurements for ocean wind field applications. In other words, the sensitivity of wind speed and direction versus the microwave frequency should

be determined. Finally, the design of a polarimetric radiometer which is capable of measuring at least the first three Stokes parameters with the required accuracy and stability should be studied.

Acknowledgment. The research described in this paper was carried out by the Jet Propulsion Laboratory, under a contract with the National Aeronautics and Space Administration; and by the Massachusetts Institute of Technology sponsored by the ONR grant N00014-92-J-1616 and a National Science Foundation Graduate Fellowship.

References

- Etkin, V. S., M. D. Raev, M. G. Bulatov, Yu. A. Militky, A. V. Smirnov, V. Yu. Raizer, Yu. A. Trokhimovsky, V. G. Irisov, A. V. Kuzmin, K. Ts. Litovchenko, E. A. Bepalova, E. I. Skvortsov, M. N. Pospelov, and A. I. Smirnov, Radiohydrophysical Aerospace Research of Ocean, *Rep. IIP-1749*, Academy of Sciences, Space Research Institute, Moscow, Russia, 1991.
- Johnson, J. T., J. A. Kong, R. T. Shin, D. H. Staelin, K. O'Neill, and A. W. Lohanick, Third Stokes Parameter Emission from a Periodic Water Surface, *IEEE Trans. Geosci. Remote Sens.*, in press, 1993.
- Jones, W. L., L. C. Schroeder, D. H. Boggs, E. M. Bracalente, R. A. Brown, G. J. Dome, W. J. Peirson, and F. J. Wentz, The geophysical evaluation of remotely sensed wind vectors over the ocean, *J. Geophys. Res.*, 87, 3297–3317, 1982.
- Klein, L. A., and C. T. Swift, An improved model for the dielectric constant of sea water at microwave frequencies, *IEEE Trans. Antennas Propag.*, AP-25, 104–111, 1977.
- Naderi, F. M., M. H. Freilich, and D. G. Long, Spaceborne radar measurement of wind velocity over the ocean—An overview of the NSCAT scatterometer system, *Proc. IEEE*, 79(6), 850–866, 1991.
- Nghiem, S. V., M. E. Veysoglu, R. T. Shin, J. A. Kong, K. O'Neill, and A. Lohanick, Polarimetric passive remote sensing of a periodic soil surface: Microwave measurements and analysis, *J. Electromagn. Waves Appl.*, 5(9), 997–1005, 1991.
- Peake, W. H., Interaction of electromagnetic waves with some natural surfaces, *IEEE Trans. Antennas Propag.*, Spec. Suppl., AP-7, 8324–8329, 1959.
- Sasaki, Y., I. Asanuma, K. Muneyama, G. Naito, and T. Suzuki, The dependence of sea-surface microwave emission on wind speed, frequency, incidence angle, and polarization over the frequency range from 1 to 40 GHz, *IEEE Trans. Geosci. Remote Sens.*, GE-25(2), 138–146, 1987.
- Stogryn, A., The apparent temperature of the sea at

- microwave frequencies, *IEEE Trans. Antennas Propag.*, AP-15(2), 278–286, 1967.
- Tsang, L., Polarimetric passive remote sensing of random discrete scatterers and rough surfaces, *J. Electromagn. Waves Appl.*, 5(1), 41–57, 1991.
- Veysoglu, M. E., S. H. Yueh, R. T. Shin, and J. A. Kong, Polarimetric passive remote sensing of periodic surfaces, *J. Electromagn. Waves Appl.*, 5(3), 267–280, 1991.
- Wentz, F. J., Measurement of oceanic wind vector using satellite microwave radiometers, *IEEE Trans. Geosci. Remote Sens.*, 30(5), 960–972, 1994.
- Yueh, S. H., and R. Kwok, Polarimetric passive remote sensing of terrain surfaces, in *International Geoscience and Remote Sensing Symposium*, p. 14, IEEE, New York, 1992.
- Yueh, S. H., S. V. Nghiem, and R. Kwok, Polarimetric emission from anisotropic media for passive remote sensing of sea ice, in *Proceedings of International Geoscience and Remote Sensing Symposium*, vol. II, pp. 966–968, IEEE, New York, 1992.
-
- J. T. Johnson and J. A. Kong, Department of Electrical Engineering and Computer Science and Research Laboratory of Electronics, Massachusetts Institute of Technology, Cambridge, MA 02139.
- R. Kwok, F. K. Li, S. V. Nghiem, W. J. Wilson, and S. H. Yueh, Jet Propulsion Laboratory, California Institute of Technology, 4800 Oak Grove Drive, Pasadena, CA 91109.
- (Received December 29, 1992; revised June 23, 1993; accepted July 2, 1993.)